DOI: 10.1021/ma100150j

Macromolecules
ARTICLE

Thickness Dependence of Neutral Parameter Windows for Perpendicularly Oriented Block Copolymer Thin Films

Hyo Seon Suh,[†,‡] Huiman Kang,[§] Paul F. Nealey,[§] and Kookheon Char*[,†,‡]

[†]*Interdisciplinary Program in Nano-Science and Technology, and* [‡]*Center for Functional Polymer Thin Films and School of Chemical and Biological Engineering, Seoul National University, Seoul, 151-744, Korea, and* [§]*Department of Chemical and Biological Engineering, University of Wisconsin-Madison, Madison, Wisconsin 53706, USA*

Received January 20, 2010; Revised Manuscript Received April 19, 2010

ABSTRACT: Balancing the interfacial interactions of a block copolymer (BCP) with a substrate as well as the free surface could induce the perpendicular orientation of microdomains, allowing the BCP films to serve as templates for nanofabrication. However, it has been observed that such perpendicular orientation of BCP microdomains is quite sensitive to the film thickness. We investigated the effect of film thickness on the orientation of microdomains in lamellae-forming P(S-*b*-MMA) thin films placed on thermally cured organosilicate (OS) substrates. For the film thickness of P(S-*b*-MMA) ranging from 1.25 L_0 up to 2.5 L_0, we varied the surface energy of the OS substrate around the value close to the energetically neutral condition by controlling the substrate cure temperature. We demonstrate the origin of the observed thickness effect by taking into account the increase in surface area at the free surface when the P(S-*b*-MMA) films make holes or islands depending on the incommensurate conditions of the BCP film. This simple but quantitative analysis allows us to define more accurate neutral windows for P(S-*b*-MMA) thin films in terms of both substrate surface energy and BCP film thickness.

Introduction

The block copolymer (BCP) thin films have recently been considered as useful templates for nanolithography because well-defined periodic nanopatterns can be realized by the simple coating process based on the self-assembly of the BCP materials.[1−7] For practical applications of such BCP thin films, the phase-separated microdomains in BCP thin films should be perpendicularly oriented with respect to supporting substrates. However, the energetically favorable interactions of one block of BCP at the interfaces typically lead to the parallel orientation of microdomains with respect to the substrate.[8−10] Thus, in order to obtain the perpendicularly oriented BCP thin films, the preferential interactions of one of the BCP block at the interfaces need to be prevented. Several approaches to realize the nonpreferential wetting substrates have been reported such as the modification of supporting substrates with random copolymer brushes or mats,[11−16] self-assembled monolayers (SAMs),[17,18] and the use of surface energy-tunable organosilicate (OS) substrates.[19] These approaches allow the BCP films to form the energetically favorable perpendicular orientation of BCP microdomains on the neutralized substrates by controlling the surface energy of the substrates.

In addition to the surface energy (or energetic consideration) of substrates, the thickness of BCP films also affects the orientation of BCP microdomains. It has been well-known that the perpendicular orientation, particularly for relatively thick BCP films placed on energetically neutral substrates, suffers from the parallel orientation induced by the preferential segregation of one block at the free surface even at a slight difference in surface energy when compared with the other block.[20,21] Therefore, the perpendicular orientation from an energetically neutral substrate was believed to propagate up to a certain distance from the substrate. However, a few observations have recently been made such that the perpendicular orientation does not simply diminish as the distance from the substrate is increased. Yager et al.[22] reported that the perpendicular orientation of P(S-*b*-MMA) films placed on a substrate containing partially coated nanoparticles can be observed in a specific thickness range of the BCP films, and the thickness range showing the perpendicular orientation oscillates with a period of L_0 (the domain spacing of a given BCP) in the BCP film thickness. In addition, Han et al.[23] also reported the similar result. On the substrates modified with slightly PMMA-preferential random copolymer brushes, the relatively thick P(S-*b*-MMA) films annealed at 230 °C can be oriented perpendicular except when the thickness of BCP film is around $(n + {}^1/_2)L_0$, where n is an integer number. Their observations indicate that although the roughness of substrates and the relevant annealing temperature would facilitate the BCP films to be oriented perpendicularly, the perpendicular orientation of BCP microdomains is inhibited by the commensurate thickness of the BCP films. Consequently, once they changed the film thickness from the commensurate thickness, they could observe the perpendicular orientation even with thicker BCP films.

To successfully realize the perpendicular orientation of microdomains in BCP films in large area, this effect of the commensurate thickness on the orientation of BCP microdomains should be understood in more detail together with the effects of other parameters such as the surface energy of substrates, the roughness of substrates, and the annealing temperature. Among these parameters, the first essential parameter set to be studied is a set of the surface energy of a substrate and the thickness of a BCP film because the influence of other parameters on the orientation of BCP microdomains can be additionally considered on the basis of the study with this set. Ham et al.[24] studied such a basic parameter set for the perpendicular orientation of BCP microdomains

*E-mail: khchar@plaza.snu.ac.kr. Telephone: +82-2-880-7431. Fax: +82-2-873-1548.

 Published on Web 04/26/2010

Table 1. Estimation of Surface and Interface Energies Obtained from the Contact Angle Experiments on OS Substrates Cured at Different Temperatures Ranging from 260 to 340 °C

cure temperature of OS substrate (°C)	contact angle of water (deg)	contact angle of diiodomethane (deg)	γ_{OS}[a] (mJ/m^2)	$\gamma_{PS\text{-}OS}$[b] (mJ/m^2)	$\gamma_{PMMA\text{-}OS}$[b] (mJ/m^2)
260	79.3 ± 1.7	61.2 ± 0.3	37.95 ± 0.72	2.55 ± 0.38	0.28 ± 0.04
280	82.4 ± 0.1	62.9 ± 0.3	36.01 ± 0.09	2.17 ± 0.05	0.37 ± 0.02
300	84.8 ± 0.2	63.2 ± 0.5	34.88 ± 0.18	1.80 ± 0.10	0.51 ± 0.03
320	90.3 ± 0.1	64.0 ± 0.2	32.42 ± 0.08	1.36 ± 0.03	1.27 ± 0.03
340	93.5 ± 0.2	64.5 ± 0.1	31.09 ± 0.07	1.39 ± 0.02	2.05 ± 0.04

[a] Surface energy values of the OS substrates were estimated based on the two liquid (water and diiodomethane as contacting liquids) harmonic method.[26−28] [b] Interfacial energy values between OS substrates and each block of P(S-*b*-MMA) were estimated by the harmonic mean equation. The surface energy values of PS and PMMA blocks used in the estimation: $\gamma_{PS} = \gamma_{PS}^{d} + \gamma_{PS}^{p} = 33.9 + 6.8 = 40.7$ (mJ/m^2), $\gamma_{PMMA} = \gamma_{PMMA}^{d} + \gamma_{PMMA}^{p} = 29.6 + 11.5 = 41.1$ (mJ/m^2).[29]

based on the surface energy of a substrate and the thickness of a BCP film. However, their parameter windows for relatively thin BCP films (~1 L_0) cannot reflect the effect of the commensurate thickness on the orientations of microdomains, which could be observed with much thicker BCP films. Furthermore, to quantitatively address the effect of the commensurate thickness, the BCP film thickness should be selected on the basis of the commensurate thickness of a given BCP.

In present study, we demonstrate the commensurate thickness-dependent parameter windows that precisely predict the wetting behavior as well as the microdomain orientation of BCP films. To investigate the effect of the surface energy of substrates, we placed P(S-*b*-MMA) films on surface energy-tunable OS substrates. The surface energy of the OS substrates was varied around the value close to the energetically neutral condition against PS and PMMA blocks. The thickness of BCP films on these OS substrates was systematically controlled and increased from 1.25 L_0 up to 2.5 L_0. Within the thickness range we studied, we found that the orientation of BCP films was dominated by the energy penalties originating from the free surface of the BCP films. The quantitative analysis of these penalties allows us to define more accurate parameter windows for P(S-*b*-MMA) thin films in terms of both the substrate surface energy and the BCP film thickness.

Experimental Section

Materials. OS used as the bottom substrate was synthesized by the sol−gel reaction with methyltrimethoxysilane (MTMS, Aldrich) and 1,2-bis(trimethoxysilyl)ethane (BTMSE, Aldrich). The detail synthetic procedure is described elsewhere.[25] The feed ratio of MTMS and BTMSE was 9/2 by mol %. 104 kg/mol (52k-52k) PS-*b*-PMMA and 3.7 kg/mol monohydroxy terminated polystyrene were purchased from Polymer Source Inc. and used without further purification. The lamellae domain spacing (L_0) of BCP is 48 nm.

Preparation of Substrates. The 100 nm thick OS films were prepared by spin coating with 5 wt % of OS solutions dissolved in methyl isobutyl ketone (MIBK) onto clean Si wafers. The OS substrates were cured at desired temperature for 6 h with a high vacuum chamber to control the surface energy of OS substrates. The bare Si wafers cleaned with piranha treatment were used as the substrates selectively wetted by the PMMA block. The PS wetting substrates were prepared by grafting monohydroxy-terminated polystyrene (PS brush) onto the Si wafers. The 40 nm thick monohydroxy-terminated polystyrene films were prepared by spin coating with 1 wt % of monohydroxy-terminated polystyrene solution dissolved in toluene and then annealed at 170 °C for 48 h under vacuum to graft PS brushes onto the Si wafers. Unreacted polymers were removed by repeated sonication in toluene at 40 °C for 3 min.

Preparation of BCP Films. On the substrates prepared by above methods, P(S-*b*-MMA) films were spin-cast from the solutions of P(S-*b*-MMA) in toluene. We varied the concentration of P(S-*b*-MMA) solutions from 1.5 to 3 wt % and spin rate from 2000 to 4000 rpm to control the thickness of P(S-*b*-MMA) films from 1.25 to 2.5 L_0. The thicknesses of BCP films were checked with the ellipsometry on the BCP films deposited on the bare Si wafers. Thickness was measured after drying the film at room temperature for 24 h in the vacuum. The BCP films placed on the substrates were annealed at 190 °C for 3 days in the vacuum.

Characterizations. The surface morphologies of BCP thin films were obtained with a Field Emission-Scanning Electron Microscope (FE-SEM, LEO 1550-VP, and JSM-7401F), an Atomic Force Microscope (AFM, Digital Instrument, Nanoscope IIIA) in tapping mode and an optical microscope (Carl Zeiss, Axio Imager A1m). The thickness of BCP thin films were measured with a variable-angle multiwavelength ellipsometer (Gaertner, L2W15S830) with two wavelengths at 633 and 834.5 nm. Static contact angles of water and diiodomethane on thermally cured OS substrates were measured using a drop shape analysis system (Kruss, DSA 100). The analyses of optical microscope images were carried out with an Image-Pro Plus software (Media Cybernetics Inc.).

Results

We have previously reported the neutral OS substrates which can orient the microphase-separated domains of P(S-*b*-MMA) films perpendicular to the OS substrates.[19] It has been well documented that the surface energy of the OS substrate could be finely controlled by cure temperature determining the relative amount of hydrophilic silanol groups in the OS substrate. Because of such tunability of the surface energy, we were able to balance the interfacial interactions of both PS and PMMA blocks against the OS substrate, leading to the perpendicularly oriented BCP films on the OS substrates. In the present study, we treated the same OS substrates in a high vacuum chamber instead of a nitrogen purging furnace used in the previous study. Since the surface energy of OS substrates would be finely varied by the cure protocol, the surface energy of OS substrates depends not only on the cure temperature but also on the other conditions such as atmosphere during the cure process and a type of annealing equipment. Thus, the OS substrates thermally treated in this study yield slightly different surface energies when compared with the surface energies given in the previous study (see Table 1). We, however, could observe the same tendency that the surface energy of OS substrates decreases as the cure temperature is increased. As a result, we were able to identify the new neutral cure temperature enabling the interfacial energies of both blocks against the OS substrate to be almost identical in this cure protocol. As noted from Table 1, the cure temperature to realize the energetically neutral OS substrate for the P(S-*b*-MMA) used in present study was around 320 °C.

As mentioned in the Introduction, we intended to investigate the combined effect of the surface energy of a bottom OS substrate as well as the BCP film thickness on the orientation of microdomains of a BCP thin film. In order to investigate such combined effect, we deposited the P(S-*b*-MMA) films with

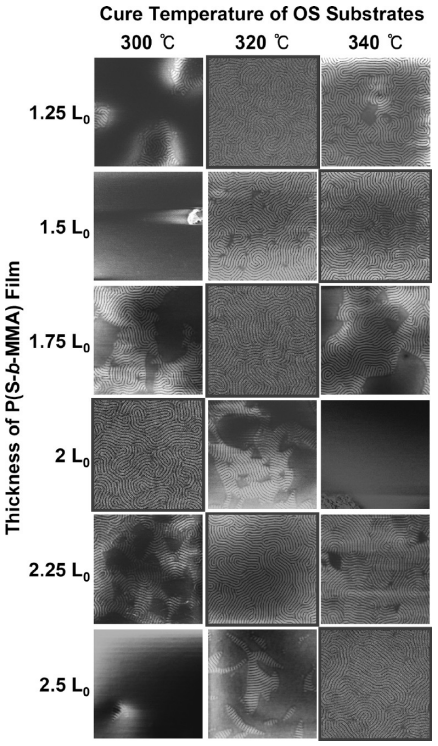

Figure 1. FE-SEM images of thermally annealed P(S-*b*-MMA) films with different thickness placed on the OS substrates cured at different temperatures ranging from 300 to 340 °C. Conditions for the energetically neutral substrates showing the perpendicular orientation of P(S-*b*-MMA) films vary as the film thickness of the P(S-*b*-MMA) is increased. Note that the size of all the FE-SEM images in the figure is 2 μm × 2 μm.

thicknesses ranging from 1.25 to 2.5 L_0 on the OS substrates cured at different temperatures ranging from 300 to 340 °C. Changing the cure temperature from 320 °C allows us to prepare the OS substrates slightly off the neutral condition in terms of the surface energy. For example, the OS substrate cured at 300 °C (**OS300**) is slightly off-neutral toward the PMMA-preferential wetting whereas the OS substrate cured at 340 °C (**OS340**) is slightly off-neutral toward the PS-preferential wetting. From the viewpoint of the surface energy, the increase in cure temperature for OS substrates in this study is similar to the increase in styrene fraction in P(S-*r*-MMA) brushes or mats.[23,24,30] We need to ensure that the surface roughness of OS substrates is not a contributing factor in the present study because the surface roughness of OS substrates do not vary much depending on cure temperature and those values are also significantly smaller than the substrate roughness affecting the orientation of BCP films[22,31] (rms roughness of **OS300**, **OS320**, and **OS340** measured by AFM is 0.373, 0.455, and 0.487 nm, respectively). Upon annealing the BCP films at different thicknesses on different sets of OS substrates (**OS300**, **OS320**, and **OS340**) at 190 °C for 3 days, we obtained the top down FE-SEM images of BCP films shown in Figure 1.

As shown in Figure 1, the orientation of microdomains in the BCP films is quite sensitive to the surface energy of OS substrates as well as the BCP film thickness. Such thickness effect on the orientation of BCP films placed on each OS substrate can be clearly appreciated by quantifying the surface fraction of perpendicular regions as a function of BCP film thickness, as shown in Figure 2. The fraction of perpendicular regions was obtained by the image analysis. On the surface of **OS300**, one can observe the perpendicular orientation of BCP microdomains only when the BCP film thickness is equivalent to nL_0 (n is the integer number) while the parallel orientation of microdomains is observed when the BCP film thickness is related to $(n + {}^1/_2)L_0$. In contrast, when

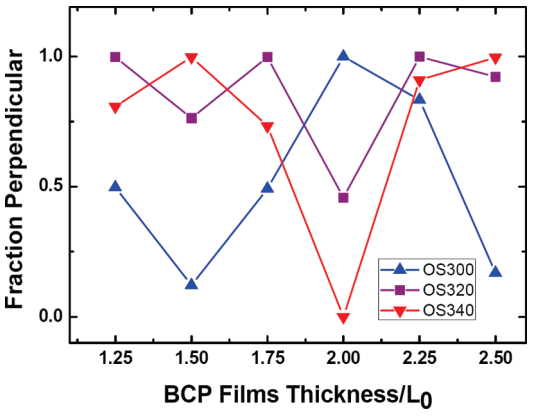

Figure 2. The surface fraction of perpendicular regions in BCP films on **OS300**, **OS320**, and **OS340** as a function of BCP film thickness. The fraction of perpendicular regions was obtained by the image analysis.

BCP films were placed on **OS340** substrates, we found the completely opposite correlation between the film thickness and the orientation of microdomains of BCP films. On both OS substrates (**OS300** and **OS340**), we also note that only partial fractions of perpendicularly oriented microdomains are observed when the BCP film thickness is equivalent to $(n \pm {}^1/_4)L_0$.

This result showing the commensurate thickness effect on the microdomain orientation is similar to other results previously reported.[22,24] On a substrate containing PMMA-preferential nanoparticles, the fraction of perpendicular lamellae of BCP films can be maximized when the films thickness is nL_0 whereas that fraction is minimized when the thickness is $(n + {}^1/_2)L_0$,[22] which is the similar result shown on a slightly PMMA-preferential **OS300** in present study. Similarly, on the substrates modified with random copolymer brushes with lower PS mole fraction (i.e., slightly PMMA-preferential substrates), the perpendicular orientation of lamellae domains was observed when the film thickness is around L_0 (29.4 nm for a given BCP),[24] which is again in good agreement with the result on a **OS300** substrate. In contrast, on the slightly PS-preferential substrates modified with random copolymer brushes with higher PS mole fraction, the perpendicular orientation of lamellae domains was observed when the film thickness is around 0.5 L_0,[24] which is in good agreement with the result obtained from a slightly PS-preferential **OS340**.

Interestingly, on top of the **OS320** substrate, which is believed to be the most energetically neutral OS substrate for a given BCP, the perfect perpendicular orientation of microdomains is observed with the film thickness equivalent to $(n \pm {}^1/_4)L_0$. We, however, observe that although the **OS320** substrate is considered to be the most neutral substrate, several defects in the perpendicularly oriented BCP films are inevitable when the BCP film thickness is either nL_0 or $(n + {}^1/_2)L_0$, which is the BCP film thickness that induces the perpendicular orientation of microdomains on **OS300** and **OS340** substrates, respectively. Although we thermally treated the OS substrates with 10 °C temperature gap from 300 to 340 °C, we failed to find any OS substrate showing the thickness-independent perpendicular orientation of BCP domains on the OS substrate. The message we can take at the moment is the fact that the substrate showing the perpendicular orientation of BCP microdomains varies as the thickness of BCP films is increased.

Discussions

Changes in Total Interfacial Energy of BCP Films Depending on Film Thickness. We believe that the shift in surface energy (or the cure temperature of OS substrates) window for

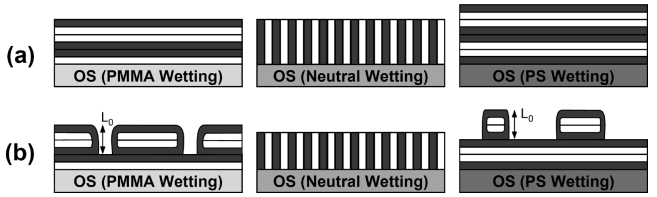

Figure 3. Schematics on the orientation of P(S-*b*-MMA) thin films with (a) commensurate and (b) incommensurate film thicknesses on the PMMA preferential wetting/energetically neutral wetting/PS preferential wetting on OS substrates (from left to right). White sections in the schematic represent the PMMA blocks while the dark gray regions represent the PS blocks.

the perpendicular orientation of BCP microdomains depends on the commensurate thickness of a BCP films. To demonstrate the effect of BCP film thickness on the orientation of microdomains, we focus on the total interfacial energy (γ_{total}) of a BCP film placed on an OS substrate. γ_{total}, in the present study, refers to the sum of interfacial energies at both bottom and top surfaces of a BCP film. γ_{total} of a BCP film placed on an OS substrate is determined by wetting blocks on the OS substrate and the exposed blocks at the top surface of the film. As shown in Figure 3a, when the BCP films with commensurate thicknesses show the parallel orientation of microdomains due to the preferential wetting of one of the blocks on the OS substrate, the PS blocks typically occupy the top surface of the BCP film originating from its lower surface energy compared with that of the PMMA block. Consequently, the γ_{total} of BCP films in these cases is

$$\gamma_{total} = \gamma_{PMMA-OS} + \gamma_{PS}$$
(PMMA preferential wetting on OS substrate with $t_{BCP} = (n+1/2)L_0$) (1)

$$\gamma_{total} = \gamma_{PS-OS} + \gamma_{PS}$$
(PS preferential wetting on OS substrate with $t_{BCP} = nL_0$) (2)

where t_{BCP} is the BCP film thickness. In these cases, the surface energy of the BCP film at the free surface is equal to the surface energy of the PS block (γ_{PS}).

In the case of BCP films with the perpendicular orientation of microdomains, both PS and PMMA blocks wet on the OS substrate and, at the same time, are exposed at the top surface with equal area fraction due to the symmetry of microdomains of the lamellae-forming BCP. Therefore, the γ_{total} in this case is

$$\gamma_{total} = \frac{1}{2}(\gamma_{PS-OS} + \gamma_{PMMA-OS}) + \frac{1}{2}(\gamma_{PS} + \gamma_{PMMA})$$
(for energetically neutral wetting) (3)

However, when the BCP film thickness deviates from the commensurate film thickness, the γ_{total} of BCP films with the parallel orientation of microdomains on selectively wetting substrates, as shown in eqs 1 and 2, should be modified to take into account the holes and islands (or bicontinuous structure) formed at the top free surface. As shown in Figure 3b, the bumpy morphological features of the BCP films in this case increase the surface area at the free surface of BCP films. As a result, the surface energy at the free surface of a BCP film also increases as the surface area is increased. If we let α denote the relative increase in surface area at the free surface of a BCP film with respect to unit flat area, the γ_{total} in these cases becomes:

$$\gamma_{total} = \gamma_{PMMA-OS} + (1+\alpha)\gamma_{PS}$$
(PMMA preferential wetting on OS substrate with $t_{BCP} \neq (n+1/2)L_0$) (4)

$$\gamma_{total} = \gamma_{PS-OS} + (1+\alpha)\gamma_{PS}$$
(PS preferential wetting on OS substrate with $t_{BCP} \neq nL_0$) (5)

In the case of the perpendicularly oriented BCP films with equivalent incommensurate film thicknesses, on the other hand, the γ_{total} value dose not change from eq 3 because the surface area at the flat free surface of the BCP films remains the constant. It is noteworthy that the γ_{total} of BCP films with perpendicular orientation dose not change while the γ_{total} of BCP films with parallel orientation varies because of the α values that change as a function of BCP film thickness.

To predict the most favorable wetting as well as the microdomain orientation of a BCP film with a specific thickness on an OS substrate, we are required to find out the lowest γ_{total} value of a BCP film among the three possible wetting cases (PMMA preferential, energetically neutral and PS-preferential wetting). In other words, we have to compare the γ_{total} values given by eqs 4, 3, and 2 for a BCP film with film thickness of nL_0, while the γ_{total} values given by eqs 1, 3 and 5 for a BCP film with film thickness of $(n+{}^1/_2)L_0$. Except these two cases, we need to compare the γ_{total} values represented by eqs 4, 3 and 5.

Estimation of α Values. To estimate the α values introduced in eqs 4 and 5, we experimentally measured the increase in surface area at the free surface of BCP films for each wetting case at a specific BCP film thickness. On nonselective (or energetically neutral) substrates such as the OS substrates in this study, however, the hole and island structures are typically not formed such that the increase in surface area at the free surface cannot be directly estimated. As a result, we deposited and annealed the BCP films with controlled thickness ranging from 1.25 to 2.5 L_0 on either bare Si wafers or Si wafers modified with PS brushes, which were considered to be the ideal substrates for PMMA- and PS-preferential wetting, respectively. As shown in Figure 4, we observe holes, islands, and bicontinuous structures with OM and AFM at the free surface of the BCP films deposited on both substrates except with the BCP films with commensurate film thicknesses for each substrate. If we assume that these holes or islands observed have the ideal shape of disks, the increased area at the free surface of a bumpy BCP film is equal to the sum of sidewall areas of these disk structures. The sum of sidewall areas can be estimated by multiplying the sum of perimeters of these disks with the height of the disk, which is known to be L_0 (48 nm) in this case, as confirmed by AFM. The sum of perimeters was obtained from the OM images shown in Figure 4, parts a and c, using the image analysis software (see the Supporting Information) and those values are listed in Table 2 for each case with different substrates and film thicknesses. We then estimated the α values by dividing the sum of sidewall areas by the area of the analyzed OM image, typically 62.4 μm × 62.4 μm and those values are also listed in Table 2. According to our estimation, the surface area at the free surface of bumpy BCP films for each case we have examined

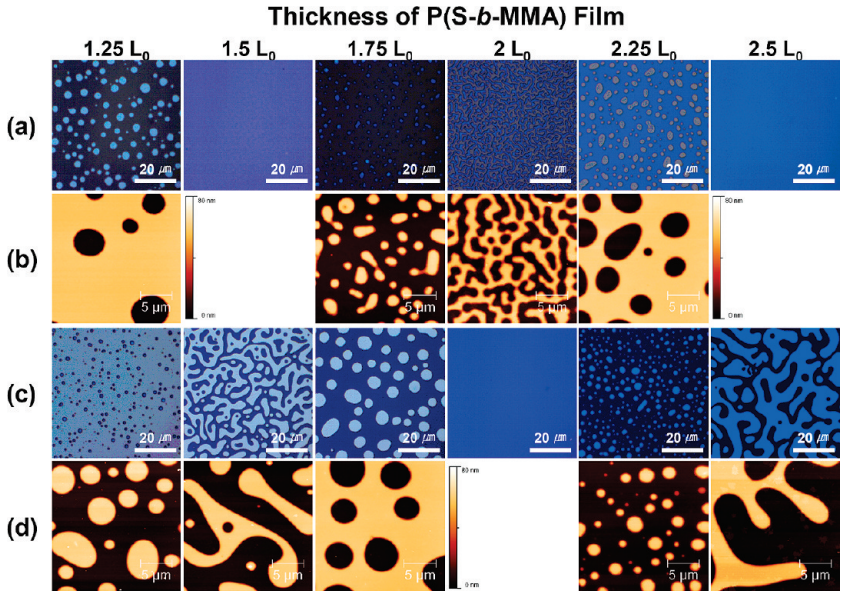

Figure 4. (a, c) Optical microscope images and (b, d) AFM height images of thermally annealed P(S-*b*-MMA) films with controlled film thicknesses on bare Si wafers (a, b) and Si wafers modified with PS brushes (c, d).

Table 2. Estimation on the Increase in Surface Area at the Free Surfaces of Asymmetric and Symmetric Wetting P(S-*b*-MMA) Films

	thickness of P(S-*b*-MMA) film for SI wafer or PS brush substrate											
	1.25 L_0		1.5 L_0		1.75 L_0		2 L_0		2.25 L_0		2.5 L_0	
parameter	Si wafer	PS brush	Si wafer	PS brush	Si wafer	PS brush	Si wafer	PS brush	Si wafer	PS brush	Si wafer	PS brush
$\sum$ perimeter of islands (or holes) (μm)	922.4	1009.2		1639.8	1385.5	868.9	3598.8		1357.1	1224.2		1403.6
$\sum$ sidewall area of islands (or holes) (μm^2)	48.44	44.28		78.7	66.5	41.7	172.7		65.1	58.8		67.4
α ($\times 10^{-2}$)	1.24	1.14		2.02	1.71	1.07	4.44		1.67	1.51		1.73

increases by less than 4.5% when compared with the flat film cases.

When we estimate the α values above, we simplified holes and islands as ideal disks. In addition, we assume that all the surfaces of a parallel-oriented BCP film are covered by the PS layer. However, in the real case of hole and island structures, gradual slopes at the edges of either holes or islands were experimentally observed.[32] Moreover, it is known that the side walls of such edges have both PS and PMMA blocks exposed to the free surface. To exactly estimate the energy penalty at the free surface of parallel-oriented BCP films, we have to consider such detailed structures at the edge of hole and islands. However, the width of step (i.e., usually less than 0.2 μm[32]) is much smaller than the diameters of holes or islands (i.e., 2−5 μm in the present study). In this case, we expect that the α values would not significantly change although we take into account such shapes in the calculation. In addition, the difference in the surface energy between PS and PMMA blocks is also small and, consequently, the increase in the surface energy due to the PMMA domains exposed to the free surface of the edges would not be very significant.

Shift in Neutral Parameter Windows for Perpendicularly Oriented BCP Films. Despite the small α values, we discovered that the value of γ_{total}, which determines the orientation and the wetting behavior of BCP films, is significantly influenced by α when we took into account the surface energy at the free surface of BCP films. The γ_{total} value for each wetting and BCP film thickness is calculated based on the parameters given in Tables 1 and 2 along with relevant equations for γ_{total} for a given BCP film thickness. The results of γ_{total} values plotted against cure temperature for OS substrates are shown in Figure 5 for 3 preferred wetting cases with several BCP film thicknesses.

In the case of perpendicularly oriented BCP films, the γ_{total} values remain constant independent of BCP film thickness, as noted from Figure 5. However, the γ_{total} values for the parallel-oriented BCP films are increased by $\alpha\gamma_{PS}$ from the γ_{total} values given in the case of BCP films with flat top surface. As shown in Table 2, these α values reach the maximum when the BCP film thickness is close to the most incommensurate thickness (nL_0 for the PMMA-preferential wetting and $(n + {}^1/_2)L_0$ for PS-preferential wetting) and the α value oscillates with a period of L_0 in the BCP film thickness. Because of the thickness-dependent oscillation of the α value, the neutral cure temperature for OS substrates, which let the neutral wetting more favorable than the PS- or PMMA-preferred wetting case, also oscillates between 300 and 340 °C with a period of L_0 in the BCP film thickness.

We found that the oscillation of neutral parameter windows, shown as the purple regions in Figure 5, exactly reflects the preferred orientation of BCP microdomains on OS substrates shown in Figure 1. For example, the perpendicular orientation is preferred on the OS substrate cured at a temperature within the neutral window because the γ_{total} value for the energetically neutral wetting cases becomes lower than the other possible cases for the parallel orientation of BCP microdomains on the same OS substrate. On the OS substrates cured at 20 °C lower than the neutral window, the γ_{total} values for the neutral wetting and the PMMA-preferential wetting become close together. In contrast, on

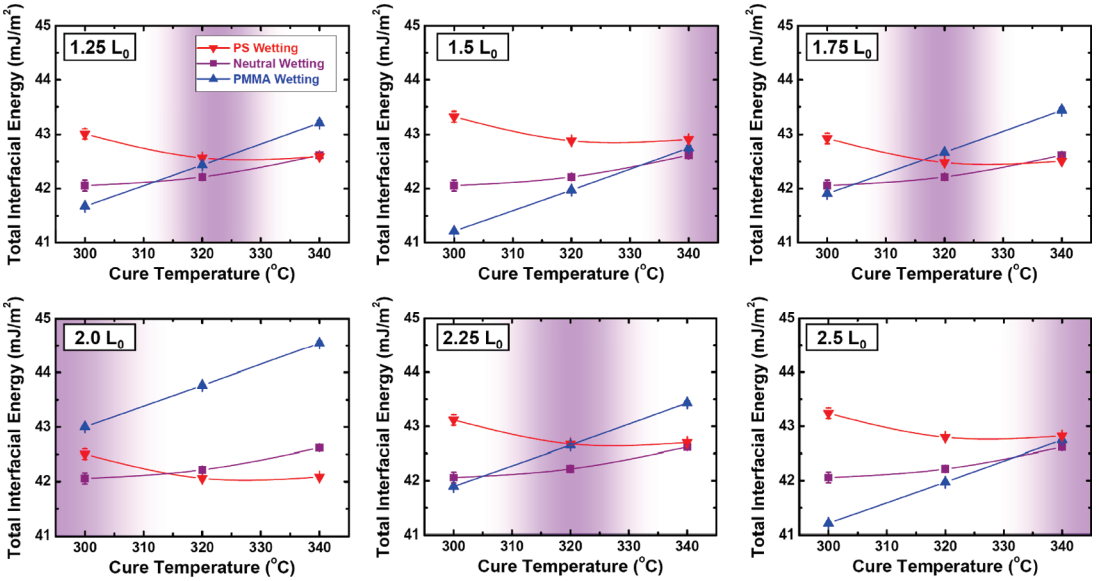

Figure 5. Total interfacial energies of P(S-*b*-MMA) films with PS-preferential wetting (▼, red), neutral wetting (■, purple), and PMMA-preferential wetting (▲, blue) on OS substrates plotted against the cure temperature of the OS substrate at different thicknesses of P(S-*b*-MMA) thin films. Note that the cure temperature to obtain energetically neutral OS substrates (shown as the purple regions in the plots) oscillates with a period of L_0 in BCP film thickness.

the OS substrates cured at 20 °C higher than the neutral window, the γ_{total} value for the energetically neutral wetting yields the value close to the PS-preferential wetting. In these two cases, energetically neutral wetting behavior is expected to compete with either PMMA-preferential or PS-preferential wetting behavior during thermal annealing of BCP films and, as a result, we observe BCP films with the perpendicular orientation coexisting with the parallel orientation with many defects after thermal annealing. Further deviation in the cure temperature for the OS substrate from the neutral window makes the γ_{total} value for either PMMA-preferential or PS-preferential wetting lower than the value for the neutral wetting case. Thus, BCP films placed on OS substrates cured at these temperatures yield the parallel orientation more favorable over the perpendicular orientation of BCP microdomains.

Orientation of BCP Films Inferred from Topographical Morphologies. The orientation and wetting behavior of BCP films predicted by the neutral parameter windows shown in Figure 5 can be confirmed by AFM measurements of topographical morphologies on the BCP films. The AFM height and phase images corresponding to the FE-SEM images given in Figure 1 are shown in Figure 6. From the AFM height images, we found that the BCP films placed on the **OS320** substrates only show the flat top surfaces regardless of the BCP film thickness while the BCP films placed on either **OS300** or **OS340** substrates show the topographical morphologies in BCP film with $(n \pm {}^1/_4)L_0$ thickness. Among the surface undulated BCP films, in the case of 1.25 and 2.25 L_0-thick BCP films placed on the **OS300** substrate and a 1.75 L_0-thick BCP film on the **OS340** substrate, the lower domains are occupied by the perpendicularly oriented BCP microdomains while the upper regions are dominated with a sort of defects. On the other hand, in the case of a 1.75 L_0-thick BCP film placed on the **OS300** substrate and 1.25 and 2.25 L_0-thick BCP films on the **OS340** substrates, we note that the opposite domains are occupied by either the perpendicularly oriented BCP microdomains or defects. However, in the case of 1.5, 2, and 2.5 L_0-thick BCP films placed on the **OS320** substrates, although the perpendicularly oriented microdomains coexist with the defects, no

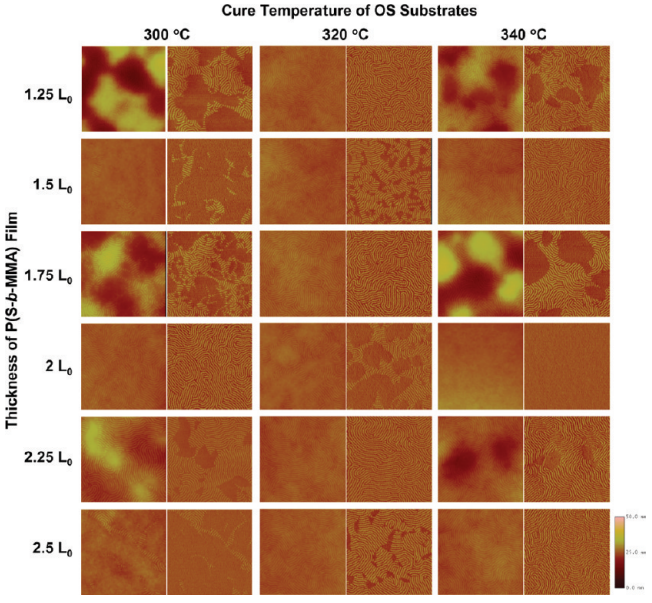

Figure 6. AFM height (left) and phase (right) images of thermally annealed P(S-*b*-MMA) films with different film thicknesses placed on OS substrates cured at different temperatures ranging from 300 to 340 °C. The size of each AFM image is 2 μm × 2 μm.

change in the film thickness is observed between those two regions.

The origin of the height difference between the perpendicularly oriented domain regions and the defect regions is the difference between the initial BCP film thickness and the commensurate film thickness for the parallel orientation of BCP microdomains, which is induced by the preferential wetting of a block competing with the neutral wetting on a specific OS substrate. In the case of 1.25, 1.75, and 2.25 L_0-thick BCP films placed on the **OS300** substrates and 1.5 and 2.5 L_0-thick BCP films deposited on the **OS320** substrates, as shown in Figure 5, the neutral wetting is in competition with the PMMA-preferential wetting with the commensurate film thickness of $(n + {}^1/_2)$ L_0. However, in the case of

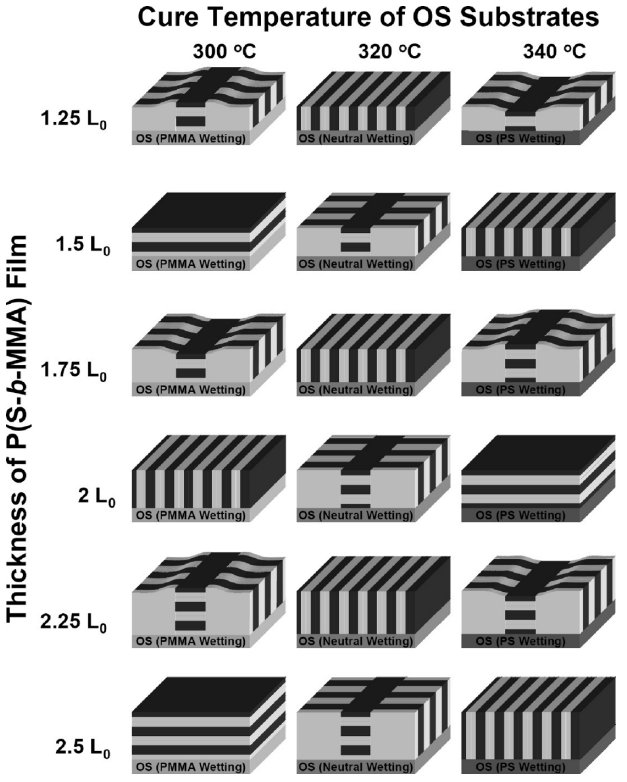

Figure 7. Schematic on the orientation of block domains of P(S-*b*-MMA) thin films at different thicknesses placed on OS substrates cured at temperatures ranging from 300 to 340 °C. The topographical morphologies shown in Figure 5 are represented.

1.25, 1.75, and 2.25 L_0-thick BCP films placed on the **OS340** substrates and a 2 L_0-thick BCP film deposited on the **OS320** substrate, the neutral wetting behavior is, in this case, competing with the PS-preferential wetting with the commensurate film thickness of nL_0. During thermal annealing of BCP films, certain regions with parallel lamellae induced by the preferential wetting behavior of BCP films would have the commensurate thickness. If the initial film thickness deviates from the commensurate thickness, the remaining regions of perpendicular lamellae become either thinner or thicker based on the mass or volume balance in the BCP film before and after annealing. Consequently, we were able to observe such height difference between the two regions. These results are summarized and also schematically shown in Figure 7. On the basis of the experimental data demonstrated in the present study, we believe that the defects, which were observed in the BCP films placed on the OS substrates cured at a temperature slightly deviating from the energetically neutral windows, are the PS block layer in the parallel orientation exposed to the top free surface. This expectation for the parallel lamellae structures in the defects is confirmed by both the top-down TEM image showing no visible microdomain in the defect regions and the cross-sectional TEM image showing clear parallel patterns coexisting with the perpendicular lamellae domains (see the Supporting Information (Figure S2)).

Grain Boundaries between Parallel and Perpendicular Lamellae Domains. During the annealing of BCP films on slightly off-neutral OS substrates, lamellae domains with both perpendicular and parallel orientations are simultaneously nucleated and grown from different locations on the same substrate, leading to the mixed morphologies. In this case, the perpendicularly oriented lamellae can intersect the edge of parallel lamellae domains with the arbitrary incidence angle. However, from the FE-SEM and AFM images of the BCP films with mixed morphologies, we found the strong preference for the perpendicular lamellae to intersect the edges of parallel lamellae at a normal angle. This preference indicates that the twist grain boundary produced by this intersection must be energetically more favorable than the tilt grain boundary produced by the perpendicular lamellae parallel to the edges of parallel lamellae domains.[33,34] In the case of tilt boundary, the interfacial morphology at the boundary is the T-junction, which is energetically unfavorable because the continuity of lamellae planes across the boundary is disrupted and thus rarely observed in the bulk samples of lamellae diblock copolymers. On the other hand, the twist boundary, observed in BCP films with mixed morphologies, generates Scherk's first surface, which is energetically more favorable due to the microphase continuity as well as the minimization of unfavorable contact between the unlike microphases. Recently, this interfacial morphology at the grain boundary has experimentally been confirmed with bulk[35] or in films[36] of diblock copolymers.

Enthalpic and Entropic Contributions in the Free Energy of BCP Films. We have so far explained the wetting and orientation behavior of BCP films placed on OS substrates based on the enthalpic contribution of free energy for given BCP films. However, in actual BCP films placed on a hard substrate, the perpendicular orientation could be more stabilized than the parallel orientation due to the entropic contribution originating from the BCP chains at such a hard substrate. Pickett et al.[37] estimated that, in the case of a lamellae forming P(S-*b*-MMA) film on a hard substrate, the order of the entropic contribution to stabilize the perpendicular orientation compared with the parallel orientation of BCP microdomains is approximately $1.6k_BT/R_z^2$, where R_z is the end-to-end distance of homopolymer constituents of the block copolymer. According to their estimation, this value for the entropic contribution is $\sim$0.2 mJ/m^2 in the case of 100 kg/mol (50K−50K) P(S-*b*-MMA), which is the similar BCP molecular weight we have used in the present study. However, the entropic energy bonus for the perpendicular orientation is several times smaller than the energy penalty from the increased surface area at the top free surface of parallel-oriented BCP films. Therefore, we expect that the neutral windows would not significantly change by taking into account such entropic effect. In addition, the excellent agreement between the simple but quantitative analysis for the neutral windows and the experimental observations convinces us that the enthalpic contribution, which significantly depends on the BCP film thickness, dominates the orientation and wetting behavior of the BCP films.

Conclusion

Using a simple but quantitative analysis for the free energy of BCP thin films, we have demonstrated how the BCP film thickness influences the orientation of BCP microdomains as well as the wetting behavior of BCP on the surface energy-tuned OS substrates. The small increase in the surface area due to the formation of holes, islands, and bicontinuous structures at the top free surface of parallel-oriented BCP films have a significant impact on the total free energy of a BCP film by the additional enthalpic contributions. With the total interfacial energy of BCP films, which reflects such additional enthalpic terms, we could almost perfectly interpret the thickness dependence of experimentally observed BCP films morphologies on the OS substrates. The quantitative analysis taken here for the additional enthalpic terms on holes, islands, and bicontinuous structures allows us to

establish the thickness dependent neutral parameter windows leading to the perpendicular orientation of BCP microdomains. The present parameter windows would give practical insights into utilizing the BCP films for many applications where the BCP film thickness plays a significant role.

Acknowledgment. This work was financially supported by the National Research Foundation of Korea (NRF) Grant funded by the Korean Ministry of Education, Science and Technology (MEST) (Acceleration Research Program (No. R17-2007-059-01000-0), NANO Systems Institute-National Core Research Center (No. R15-2003-032-05001-0), WCU (World Class University) Program (R31-10013) and graduate programs at Seoul National University through the Brain Korea 21 Program. We also acknowledge the financial support from the Korean Ministry of Knowledge Economy (MKE) on SystemIC2010 project. This work is also performed by the Collaborative Program of Nanoscale Science and Engineering Center of National Science Foundation (NSF) (DMR-0425880). We are also grateful to Heeje Woo, Sehee Kim, and Dr. Jinkee Hong for the TEM measurements.

Supporting Information Available: Figures showing typical examples of image analysis to extract perimeter data from the OM images of BCP thin films on the selectively wetting substrates and the TEM images of BCP films after removal of the supporting **OS320** substrates. This material is available free of charge via Internet at http://pubs.acs.org.

References and Notes

(1) Park, M.; Harrison, C.; Chaikin, P.; Register, R.; Adamson, D. *Science* **1997**, *276*, 1401.
(2) Harrison, C.; Park, M.; Chaikin, P. M.; Register, R. A.; Adamson, D. H. *J. Vac. Sci. Technol. B* **1998**, *16*, 544.
(3) Thurn-Albrecht, T.; Schotter, J.; Kastle, G. A.; Emley, N.; Shibauchi, T.; Krusin-Elbaum, L.; Guarini, K.; Black, C. T.; Tuominen, M. T.; Russell, T. P. *Science* **2000**, *290*, 2126.
(4) Hamley, I. W. *Nanotechnology* **2003**, *14*, R39.
(5) Park, C.; Yoon, J.; Thomas, E. L. *Polymer* **2003**, *44*, 6725.
(6) Segalman, R. A. *Mat. Sci. Eng. R-Rep.* **2005**, *48*, 191.
(7) Hawker, C. J.; Russell, T. P. *MRS Bull.* **2005**, *30*, 952.
(8) Anastasiadis, S. H.; Russell, T. P.; Satija, S. K.; Majkrzak, C. F. *Phys. Rev. Lett.* **1989**, *62*, 1852.
(9) Coulon, G.; Russell, T. P.; Deline, V. R.; Green, P. F. *Macromolecules* **2002**, *22*, 2581.
(10) Russell, T. P.; Coulon, G.; Deline, V. R.; Miller, D. C. *Macromolecules* **2002**, *22*, 4600.
(11) Mansky, P.; Russell, T. P.; Hawker, C. J.; Pitsikalis, M.; Mays, J. *Macromolecules* **1997**, *30*, 6810.
(12) Mansky, P.; Liu, Y.; Huang, E.; Russell, T. P.; Hawker, C. J. *Science* **1997**, *275*, 1458.
(13) In, I.; La, Y. H.; Park, S. M.; Nealey, P. F.; Gopalan, P. *Langmuir* **2006**, *22*, 7855.
(14) Ryu, D. Y.; Shin, K.; Drockenmuller, E.; Hawker, C. J.; Russell, T. P. *Science* **2005**, *308*, 236.
(15) Han, E.; In, I.; Park, S. M.; La, Y. H.; Wang, Y.; Nealey, P. F.; Gopalan, P. *Adv. Mater.* **2007**, *19*, 4448.
(16) Bang, J.; Bae, J.; Lowenhielm, P.; Spiessberger, C.; Given-Beck, S. A.; Russell, T. P.; Hawker, C. J. *Adv. Mater.* **2007**, *19*, 4552.
(17) Peters, R. D.; Yang, X. M.; Kim, T. K.; Nealey, P. F. *Langmuir* **2000**, *16*, 9620.
(18) Peters, R. D.; Yang, X. M.; Kim, T. K.; Sohn, B. H.; Nealey, P. F. *Langmuir* **2000**, *16*, 4625.
(19) Suh, H. S.; Kang, H.; Liu, C. C.; Nealey, P. F.; Char, K. *Macromolecules* **2010**, *43*, 461.
(20) Huang, E.; Rockford, L.; Russell, T. P.; Hawker, C. J. *Nature* **1998**, *395*, 757.
(21) Huang, E.; Mansky, P.; Russell, T. P.; Harrison, C.; Chaikin, P. M.; Register, R. A.; Hawker, C. J.; Mays, J. *Macromolecules* **2000**, *33*, 80.
(22) Yager, K. G.; Berry, B. C.; Page, K.; Patton, D.; Karim, A.; Amis, E. J. *Soft Matter* **2009**, *5*, 622.
(23) Han, E.; Stuen, K. O.; Leolukman, M.; Liu, C. C.; Nealey, P. F.; Gopalan, P. *Macromolecules* **2009**, *42*, 4896.
(24) Ham, S.; Shin, C.; Kim, E.; Ryu, D. Y.; Jeong, U.; Russell, T. P.; Hawker, C. J. *Macromolecules* **2008**, *41*, 6431.
(25) Lee, J. K.; Char, K.; Rhee, H. W.; Ro, H. W.; Yoo, D. Y.; Yoon, D. Y. *Polymer* **2001**, *42*, 9085.
(26) Wu, S. *J. Polym. Sci.* **1971**, *C34*, 19.
(27) Busscher, H. J.; Vanpelt, A. W. J.; Deboer, P.; Dejong, H. P.; Arends, J. *Colloids Surf.* **1984**, *9*, 319.
(28) van Oss, C. J. *Interfacial Forces in Aqueous Media*; CRC/Taylor & Francis: Boca Raton, FL, 2006.
(29) Wu, S. *Polymer Interface and Adhesion*; Marcel Dekker: New York, 1982.
(30) Han, E.; Stuen, K. O.; La, Y. H.; Nealey, P. F.; Gopalan, P. *Macromolecules* **2008**, *41*, 9090.
(31) Sivaniah, E.; Hayashi, Y.; Matsubara, S.; Kiyono, S.; Hashimoto, T.; Fukunaga, K.; Kramer, E. J.; Mates, T. *Macromolecules* **2005**, *38*, 1837.
(32) Carvalho, B. L.; Thomas, E. L. *Phys. Rev. Lett.* **1994**, *73*, 3321.
(33) Gido, S. P.; Gunther, J.; Thomas, E. L.; Hoffman, D. *Macromolecules* **1993**, *26*, 4506.
(34) Gido, S. P.; Thomas, E. L. *Macromolecules* **1994**, *27*, 6137.
(35) Jinnai, H.; Sawa, K.; Nishi, T. *Macromolecules* **2005**, *39*, 5815.
(36) Shin, D. O.; Kim, B. H.; Kang, J.-H.; Jeong, S.-J.; Park, S. H.; Lee, Y.-H.; Kim, S. O. *Macromolecules* **2009**, *42*, 1189.
(37) Pickett, G. T.; Witten, T. A.; Nagel, S. R. *Macromolecules* **1993**, *26*, 3194.